# We are IntechOpen,
# the world's leading publisher of
# Open Access books
# Built by scientists, for scientists

## 4,800
Open access books available

## 122,000
International authors and editors

## 135M
Downloads

Our authors are among the

## 154
Countries delivered to

## TOP 1%
most cited scientists

## 12.2%
Contributors from top 500 universities

**CLARIVATE ANALYTICS**
**BOOK CITATION INDEX**
**INDEXED**

**WEB OF SCIENCE**™

Selection of our books indexed in the Book Citation Index
in Web of Science™ Core Collection (BKCI)

# Interested in publishing with us?
# Contact book.department@intechopen.com

Numbers displayed above are based on latest data collected.
For more information visit www.intechopen.com

# Micro Power Generation from Micro Fuel Cell Combined with Micro Methanol Reformer

Taegyu Kim
*Chosun University*
*Republic of Korea*

## 1. Introduction

### 1.1 Background

Thanks to the breakthroughs in microfabrication technologies, numerous concepts of microsystems including micro aerial vehicles, microbots, and nanosatellites have been proposed. Contrary to ordinary electronic devices, these microsystems perform mechanical work and require the extended operation. As their functions are getting complex and advanced, their energy consumption is also increasing exponentially. In order to activate these microsystems, a high density power source in a small scale is required. However, present portable devices still extract power from existing batteries. The energy density of the current batteries is too low to support these microsystems (Holladay et al., 2004). Therefore, a new micro power source is essential for the successful development of new microsystems.

Various concepts for micro power generations have been introduced such as micro engines, micro gas turbines, thermoelectric generators combined with a micro combustor, and micro fuel cells. All of these concepts extract energy from a chemical fuel that have energy density much greater than that of the existing batteries. The first challenge to micro power source was the miniaturization of conventional heat engines. However, the development of micro heat engine reached a deadlock due to the difficulties of microfabrication and realization of miniaturized fast moving components and kinematics' mechanism to generate power in micro scale. Micro fuel cells have drawn attention as a primary candidate for a micro power source due to its distinctive merits that are absence of moving parts and high efficiencies. The fuel cell is an electrochemical device that directly converts chemical energy to electric energy. Due to its different energy conversion path, the fuel cell has high thermal efficiency compared to the heat engines. The energy density of the fuel cell is higher than that of the existing batteries because it uses a chemical fuel such as hydrogen (Nguyen & Chan, 2006).

There are several types of fuel cell as summarized in Table 1 (O'Hayre et al., 2006), such as polymer electrolyte membrane fuel cell (PEMFC), phosphoric acid fuel cell (PAFC), alkaline fuel cell (AFC), molten carbon fuel cell (MCFC), and solid oxide fuel cell (SOFC). Of these fuel cells, PEMFC is suitable to a micro power device due to its low operating temperature and solid phase of electrolyte. Direct methanol fuel cell (DMFC) is a kind of PEMFC except that it directly uses methanol instead of hydrogen as a fuel. Formic acid, chemical hydrides, and other alcohols can be used as a direct fuel.

|                    | PEMFC       | PAFC      | AFC      | MCFC              | SOFC           |
|--------------------|-------------|-----------|----------|-------------------|----------------|
| Electrolyte        | Polymer     | $H_3PO_4$ | KOH      | Molten carbonate  | Ceramic        |
| Charge carrier     | $H^+$       | $H^+$     | $OH^-$   | $CO_3^{2-}$       | $O^{2-}$       |
| Temperature        | 80 °C       | 200 °C    | 60-220 °C| 650 °C            | 600-1000 °C    |
| Catalyst           | Platinum    | Platinum  | Platinum | Nickel            | Perovskite     |
| Cell components    | Carbon      | Carbon    | Carbon   | Stainless         | Ceramic        |
| Fuel compatibility | $H_2$, $CH_3OH$ | $H_2$ | $H_2$    | $H_2$, $CH_4$     | $H_2$, $CH_4$, CO |

Table 1. Descriptions of major fuel cell types

In the beginning of research, DMFC has been widely investigated as a possible candidate for micro power generation due to the use of liquid fuel and its simple structure (Lua et al., 2004). However, the fuel crossover phenomena is an inherent problem of DMFC, which severely limits its power output. It is known that the power output of PEMFC is much greater than that of DMFC, and there is no fuel crossover in PEMFC. Major obstacle in the successful development of PEMFC is the difficulties of the hydrogen storage with high density. Although possible to use hydrogen in either compressed gas or liquid form, it gives significant hazards due to its explosive nature. Metal hydride suffers from high weight per unit hydrogen storage and low response for a sudden increase in hydrogen demand. Chemical storage in the form of liquid fuel such as methanol has significantly higher energy density compared to the suggested technologies. It can be reformed to generate hydrogen gas when needed. The fuel reformer is a device that extract hydrogen from a chemical fuel including methanol, methane, propane, octane, gasoline, diesel, kerosene, and so on. The fuel choice is more flexible than the direct fuel cells. Although a fuel cell combined with the reformer is more attractive, it is complex and bulky compared to the DMFC due to the fuel reformer. Therefore, the miniaturization of the reformer has been a major research activity for the successful development of PEMFC system in recent years (Pattekar & Kothare, 2004). MEMS technology is a useful tool to reduce the size of reformer and fuel cell (Yamazaki, 2004). The use of MEMS technology in a thermo-chemical system is relatively new concept. It allows the miniaturization of conventional reactors while keeping its throughput and yield. The microreactor has a relatively large specific surface area, which provides the increased rate of heat and mass transport, and short response time. In addition, MEMS-compatible materials are suitable to various chemical reaction applications due to their high thermal and chemical resistances.

## 1.2 Literature survey

Catalytic steam reforming of methanol for hydrogen production using conventional reactors has been already carried out in the literature. However, the use of microreactors is a relatively new challenge and other approaches are required for the development of micro reformers using MEMS technologies. Nevertheless, the study on the methanol reforming reaction in the conventional reactors give a good background for the development of micro methanol reformer.

Various research groups have successfully developed micro fuel reformers using MEMS technologies. Pattekar & Kothare, 2004 developed a micro-packed bed microreactor for hydrogen production, which is fabricated by deep reactive ion etching (DRIE). The width of

microchannels was 1000 μm and the depth ranged from 200 to 400 μm. The microchannels were grooved on 1000 μm thick silicon substrate using photolithography followed by DRIE. A 10 μm thick photoresist (Shipley 1045, single/dual coat) was used as a etch mask for DRIE. Commercial $Cu/ZnO/Al_2O_3$ catalyst was load by passing the water-based suspension of catalyst particles ranging from 50 to 70 μm via microchannels. The microfilter was fabricated at the end of microchannels, and the catalyst particles larger than 20 μm were trapped in the microchannels. The platinum resistance temperature detector was used as a temperature sensor with a linear temperature versus resistance characteristic. The platinum microheater was deposited along the microchannels. The methanol conversion was 88% at the steam-to-carbon ratio (S/C) of 1.5 and the methanol feed rate of 5 ml/h. The hydrogen production rate was 0.1794 mol/h that is the sufficient flow to generate 9.48 W in a typical PEMFC. Pattekar & Kothare, 2005 also developed a radial flow reactor that has less pressure drop compared to conventional one due to the increased flow cross section area along the reaction path.

Kundu et al., 2006 fabricated a microchannel reformer on a silicon wafer using silicon DRIE process. The split type channels were made in the micro vaporizer region to reduce the back pressure at the inlet port and to get a more uniform flow of fluid. The dimensions of the micro reformer were 30 mm in length and 30 mm in width, and each channel was 28 mm in length. The width of each channel was 1 mm and the depth was 300 μm. The commercial $CuO/ZnO/Al_2O_3$ catalyst (Johnson Matthey) was packed inside the channels by injecting the water-based catalyst slurry. The catalyst particles were trapped in the microchannels by filters that were in the form of 90 μm thick parallel walls spaced 10 μm apart oriented parallel to the direction of the fluid flow. The catalyst deactivation was observed after operating continuously for 8 hours using catalyst characterization. It can be seen that the performance with the serpentine channel was higher than with the parallel channel due to the longer residence time. The hydrogen production rate was 0.0445 mol/h which can produce 2.4 W assuming an 80% fuel cell operation efficiency.

Kazushi et al., 2006 developed a micro fuel reformer integrated with a combustor and a microchannel evaporator. Two fuel reforming reactors were placed on either side of a combustor to make the system compact and to use combustion heat efficiently. The silicon and Pyrex® glass wafer that are used as a substrate were stacked by anodic bonding. A commercially available reforming catalyst made of $CuO/ZnO/Al_2O_3$ (MDC-3, Süd-Chemie Catalysts Japan, Inc.) was filled into a microchamber fabricated on glass substrates after being powdered and hardened by polyvinylalcohol (PVA). The Pt loaded on $TiO_2$ support made by sol-gel method was used as a catalyst of the combustor. Thin film resistive temperature sensors made of Pt/Ti (100 nm/50 nm) to measure temperature inside the fuel reformer was fabricated on the wall of the combustion chamber by the lift-off process. The six kinds of microchannel evaporators were fabricated on the silicon substrates; as a result, it was found that the design of the microchannel evaporator is critical to obtain larger hydrogen output. The 32.9 ml/min of hydrogen, which is equivalent to 5.9 W in lower heating value, was produced when input combustion power was 11 W. The maximum efficiency of 36.3% was obtained and the power density of the reformer was 2.1 $W/cm^3$.

Though the work on the MEMS-based reformer has been continuously reported in the recent literature, there is no novel change and significant improvement. The literature could be classified into two standpoints. In terms of substrate materials, silicon wafers has been mostly used as a substrate of microreactors. Different materials have been also used such as

glass wafer, polydimethylsiloxane (PDMS), and low temperature co-fired ceramic (LTCC). In terms of a method of catalyst loading in the reactor bed, either catalyst coating or packing has been used. In almost results, the heat to sustain the methanol steam reforming reaction was provided by an external heater, while some results presented the use of a catalytic combustor as a heat source.

## 1.3 Fuel reforming process and system

Fuel reforming is a chemical process that extracts hydrogen from a liquid fuel. Fuel reformer is a device that produces hydrogen from the reforming reaction. Liquid fuel is used as a feed of the reformer due to its higher density than gaseous fuels. Considering hydrogen content and ease of reforming, methanol was chosen as the primary fuel in hydrogen sources such as alcohols and hydrocarbons (Schuessler et al., 2003).

There are a number of fuel reforming techniques available, including steam reforming (Lindström & Pettersson, 2001), partial oxidation (Wang et al., 2003), and autothermal reforming (Lindström et al., 2003). Of all considered techniques, the steam reforming process provides the highest attainable hydrogen concentration in the reformate gas. This reaction takes place at relatively low temperature in the range of 200-300 ˚C. The chemical reaction of the methanol steam reforming process is expressed below:

$$CH_3OH + H_2O \rightarrow 3H_2 + CO_2 \tag{1}$$

Equation 1 is a primary reforming process that is the stoichiometric conversion of methanol to hydrogen. It can be regarded as the overall reaction of the methanol decomposition and the water-gas shift reaction. First, the methanol decomposes to generate carbon monoxide.

$$CH_3OH \rightarrow 2H_2 + CO \tag{2}$$

The presence of water can convert carbon monoxide to carbon dioxide through the water-gas shift reaction.

$$CO + H_2O \rightarrow H_2 + CO_2 \tag{3}$$

The formation of carbon monoxide lowers the hydrogen production rate and the carbon monoxide also acts as a poison for the fuel cell catalyst. Typically, carbon monoxide is converted to carbon dioxide either in a separate water-gas shift reactor or a preferential oxidation called PROX (Delsman et al., 2004). Palladium/silver alloy membrane is also used to separate selectively the carbon monoxide. Other byproducts such as carbon dioxide and excess water vapor can be safely discharged to atmosphere.

Cu-based catalysts are used for the steam reforming of methanol, and the well-known one is $Cu/ZnO/Al_2O_3$. Generally, it has been claimed that $Cu^0$ provides catalytic activity and ZnO acts as a stabilizer of Cu surface area. Addition of $Al_2O_3$ to the binary mixture enhances Cu dispersion and catalyst stability (Agrell et al., 2003).

The steam reforming of methanol is endothermic reaction. An external electric heaters or catalytic combustors can be used as a heat sources to sustain the reforming reaction. The amount of the endothermic heat per a mole of methanol is 48.96 kJ/mol at 298 K. The electric microheater is the simplest method to supply heat to the reformer because its control is relatively easy and the fabrication can be simply integrated into MEMS process. However, the electric heater is usually used for startup period only due to its low thermal efficiency.

The catalytic combustors are an ideal alternative heat source to the electric heater because its high thermal efficiency. Methanol can be directly used in the combustor to facilitate methanol reforming reaction. Part of the hydrogen produced out of the reformer can be fed to the combustor. While it is possible that the catalytic hydrogen combustion with Pt as the catalyst even at room temperature, the methanol combustion requires preheaters to initiate the reaction. In the present study, the catalytic combustion of hydrogen and the catalytic decomposition of hydrogen peroxide were used as heat sources of the methanol steam reformer. Hydrogen peroxide as a heat source is the first attempt in the world.

Figure 1 shows the schematic of a typical reformer-combined fuel cell system, which consists of a fuel reformer and a fuel cell. The fuel reformer is classified into four units; fuel vaporizer/preheater, steam reformer, combustor/heat-exchanger, and PROX reactor. First, methanol is fed with water and is heated by the vaporizer. The methanol is reformed by the reforming catalyst to generate hydrogen in the steam reformer. To supply heat to the steam reformer, part of hydrogen from the anode off-gas of fuel cell can be fed to the combustor. The combustor generates the sufficient amount of heat to sustain the methanol reforming reaction. As mentioned before, the extremely small amount of carbon monoxide deactivates the fuel cell catalyst, which should be reduced to below 10 ppm by PROX.
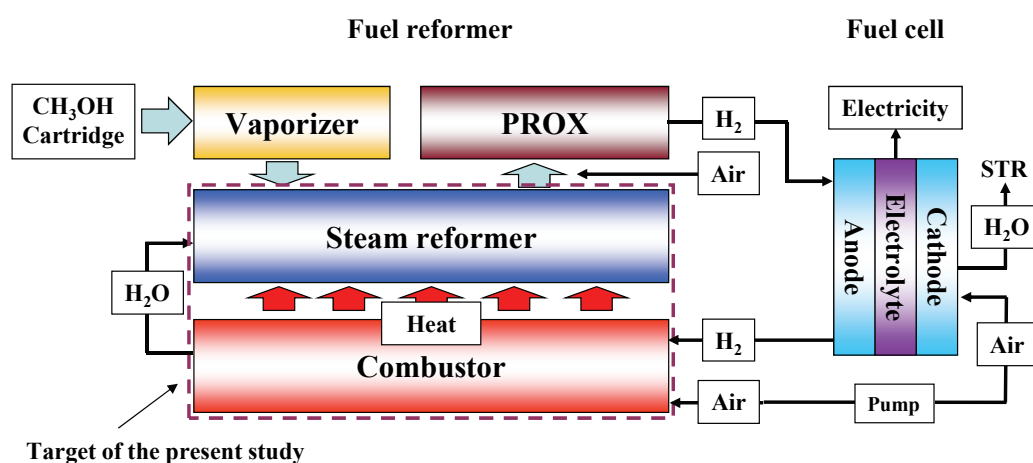


Fig. 1. Schematic of the fuel cell system combined with the fuel reformer

## 1.4 Outline of chapter

This chapter presents design, fabrication and evaluation of MEMS methanol reformer. First, a methanol reformer was fabricated and integrated with a catalytic combustor. Cu/ZnO was selected as a catalyst for the methanol steam reforming reaction and Pt for the hydrogen catalytic combustion. Wet impregnation method was used to load the catalysts on a porous support. The catalyst-loaded supports were inserted in the cavity made on the glass wafer. The performance of the micro methanol reformer was measured at various test conditions and the optimum operation condition was sought. Next, new concept of micro methanol reformer was proposed in the present study. The micro reformer consists of the methanol reforming reactor, the catalytic decomposition reactor of hydrogen peroxide, and a heat-exchanger between the two reactors. In this system, the catalytic decomposition of hydrogen peroxide is used as a process to supply heat to the reforming reactor. The decomposition process of hydrogen peroxide produces water vapor and oxygen as a product, which can be used efficiently to operate the reformer/PEMFC system. Microreactor was fabricated for

preferential oxidation of carbon monoxide using a photosensitive glass process integrated with a catalyst coating process. A $\gamma$-$Al_2O_3$ layer was coated as a catalyst support on the surface of microchannels using sol-gel method. The wet impregnation method was used to load Pt/Ru in the support. The conversion of carbon monoxide was measured with varying the ratio of oxygen to carbon ($O_2$/C) and the catalyst loading amount. Micro fuel cell was fabricated and the integrated test with the MEMS methanol reformer was performed to validate the micro power generation from the micro fuel cell system.

## 2. Micro reformer integrated with catalytic combustor

### 2.1 Design

Figure 2 depicts the construction of the integrated micro methanol reformer. The mixture of methanol and water enters the steam reformer at the top and the reformate gas leaves the reactor. The mixture of hydrogen and air flows into the catalytic combustor at the bottom with counter flow stream against the reforming stream. The heat generated from the catalytic combustor is transferred to the steam reformer through the heat-exchanger layer that has micro-fins to increase the surface area and the suspended membrane to enhance the heat transfer rate. The porous catalyst supports were inserted in the cavity made on the glass wafer as shown in Fig. 2. The micro reformer structure was made of five glass wafers; two for top and bottom, one for the steam reformer, one for the catalytic combustor, and the reminder for the heat-exchanger in-between.
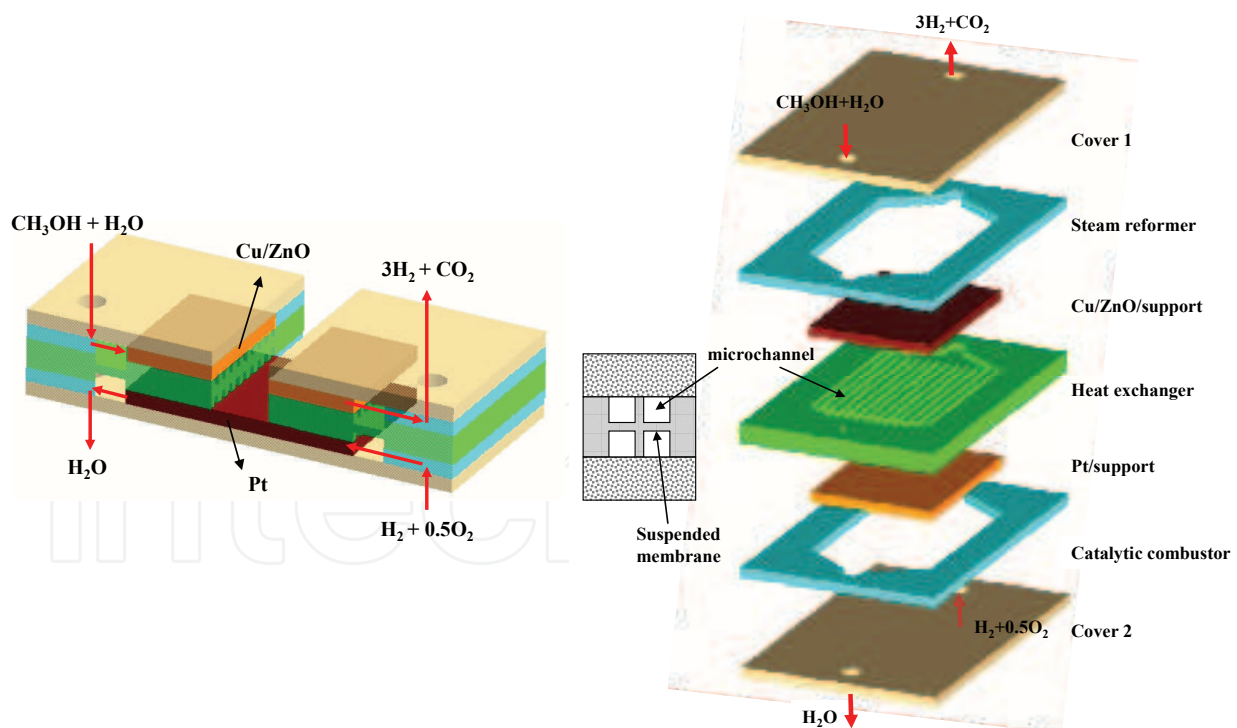


Fig. 2. Construction of the integrated micro methanol reformer

The porous ceramic material (ISOLITE®) was used as a catalyst support due to its large surface area and thermal stability (Kim et al., 2007). The typical ceramic support is composed of 40% $Al_2O_3$ and 55% $SiO_2$ with traces of the other metal oxides, and the porosity is approximately 71%. Figure 3 shows SEM images of the support material. The scale of the

bulk pores was between 100 and 300 μm, while smaller scale pores were a few microns. This structure of the porous support can enhance the heat and mass transport between catalyst active sites and reactants.
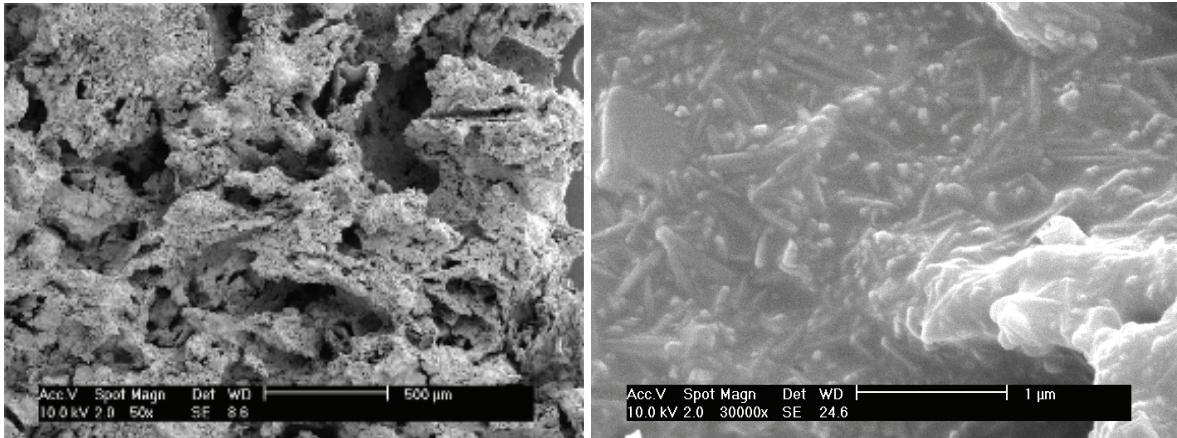


Fig. 3. SEM images of the porous ceramic material used as a catalyst support

## 2.2 Fabrication

The overall fabrication process was integrated with a catalyst loading step as shown in Fig. 4. The fabrication process for an individual glass wafer is as follows: (1) exposure to ultraviolet (UV) light under a mask at the intensity of 2 J/cm$^2$; (2) heat treatment at 585 ˚C for 1 hour to crystallize portion of the glass that was exposed to UV; and (3) etching the crystallized portion of the glass in the 10% hydrofluoric (HF) solution to result in the desired shape. The etching rate was 1 mm per hour. With step 1-3 in Fig. 4, two covers, a reformer layer, and a combustor layer were fabricated. To obtain the membrane heat-exchanger, the glass wafer was exposed by UV light on both sides of the wafer. After the heat treatment, the wafer was etched standing in the etching bath. The tooth shape cross-section of the membrane heat-exchanger layer was fabricated by controlling etching time as shown in the step 4-6 of Fig. 4. The complete micro methanol reformer was constructed by fusion-bonding the fabricated glass layers, where the porous catalyst supports were inserted in the reformer layer and the combustor layer, respectively. The best fusion-bonding between glass wafers was obtained by pressing the wafers against each other at 1000 N/m$^2$ in a furnace held at 500 ˚C (Kim & Kwon, 2006a).

As a final step, the catalysts were loaded on the porous catalyst supports. The Cu/ZnO was selected as a catalyst for methanol reforming reaction, considering its proven reactivity and selectivity (Kim & Kwon, 2006b). The Pt was chosen as a catalyst for the hydrogen catalytic combustion. The wet impregnation method was used to load both catalysts on the porous supports. A mixture of a 0.7 M aqueous solution of $Cu(NO_3)_2$ and a 0.3 M aqueous solution of $Zn(NO_3)_2$ was prepared. The mixture was injected in the catalyst support inserted in the reformer layer using a syringe pump. The moisture was removed by drying the catalyst-loaded support in a convection oven at 70 ˚C for 12 hours. Calcination procedure followed in a furnace at 350 ˚C for 3 hours. The similar procedures were used for Pt coating with 1 M aqueous solution of $H_2PtCl_6$. The amount of the loaded Cu/ZnO was 7.0 wt % while Pt was 5.0 wt % of the total weight of the catalyst support. The catalysts were reduced for 4 hours in an environment of mixture of 4% $H_2$ in $N_2$, which is steadily flowing into the reformer at a rate of 10 ml/min in a furnace of 280 ˚C.

Figure 5 shows the fabrication results, including etched glass wafers, a complete micro methanol reformer, a cross-section view of the reformer and SEM image of the membrane heat-exchanger. The total volume of the reformer was 3.6 cm$^3$ (20 mm×30 mm×6mm) and the weight was approximately 13.4 g.
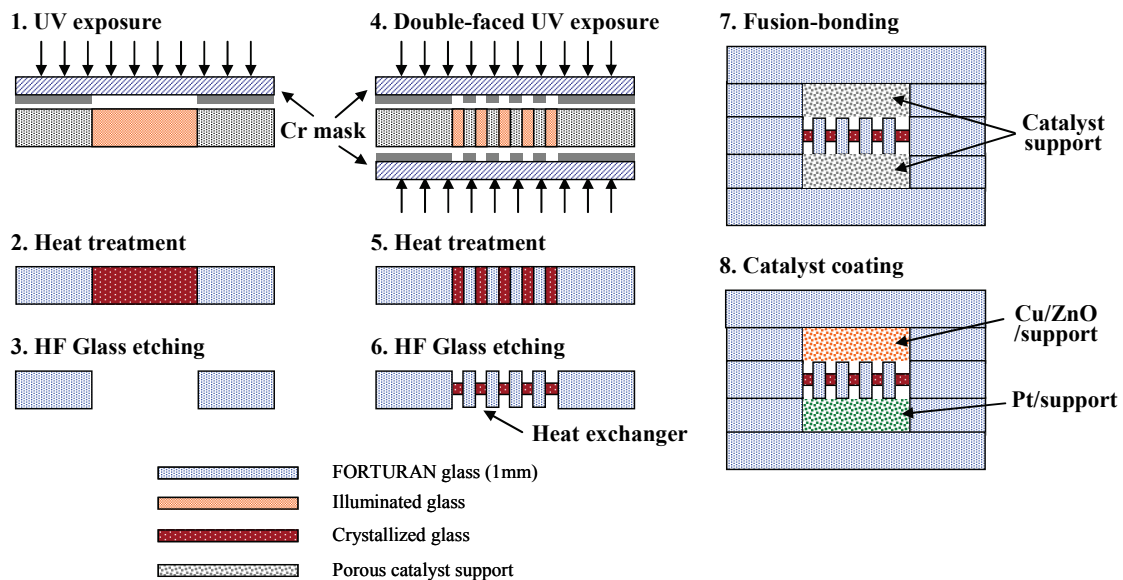


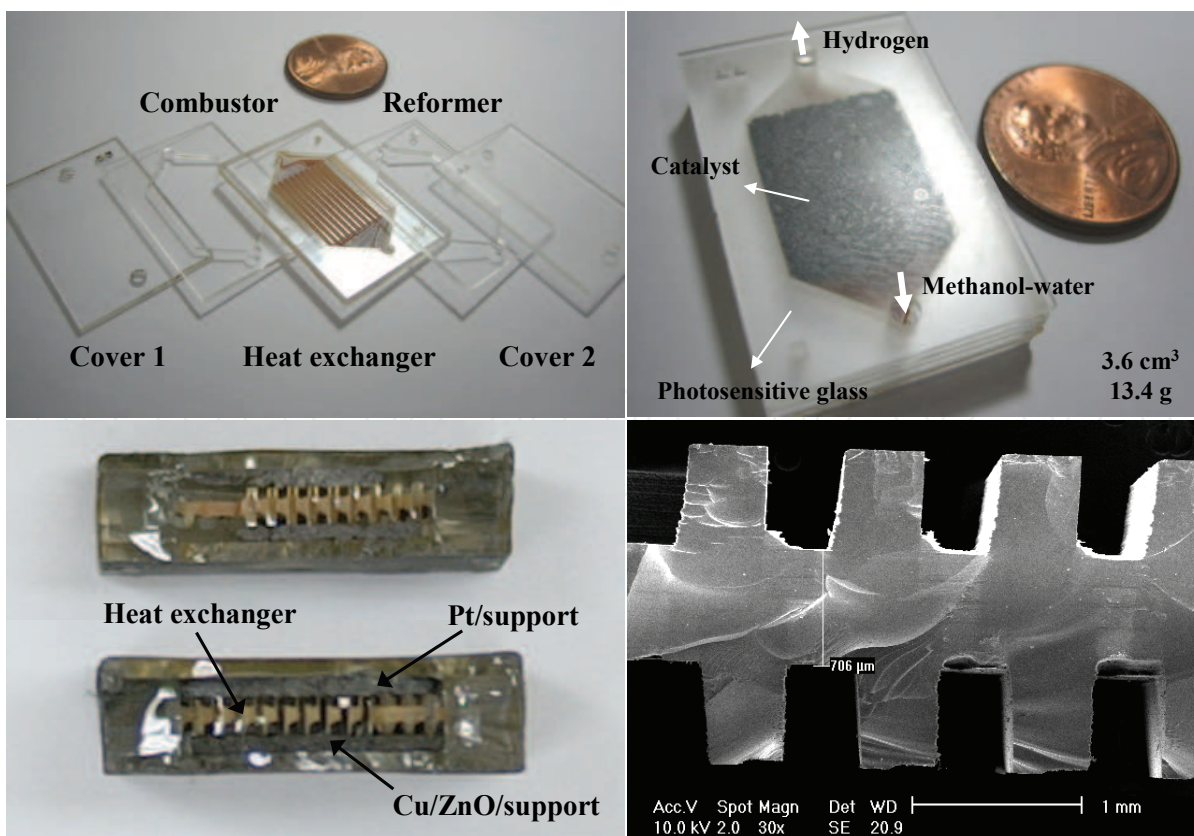Fig. 4. Overall fabrication procedure of the micro methanol reformer.



Fig. 5. Fabricated results of the micro methanol reformer

## 2.3 Performance measurement

Experimental setup was equipped to measure the performance of the micro methanol reformer. A syringe pump (KDS200, KD Scientific) supplied a mixture of methanol and water to the reformer at a controlled rate. The flow rate of hydrogen and air was controlled by mass flow controllers (EL-FLOW, Bronkhorst). After mixed them in a mixing chamber, the mixture gas was supplied to the combustor. The temperature of each reactor was recorded by thermocouples. The product gas of the reformer was cooled and the condensable portion was removed in a cold trap. The non-condensable product gas was analyzed by a gas chromatography (Agilent HP6890). The flow rate of dry gas was measured by a bubble meter. The column in the gas chromatography was Carboxen-1000 (60/80 mesh, 1/8", 18 ft) that can separate $H_2$, $N_2$, CO, $CO_2$, $CH_4$ and others. Nitrogen carrier gas at known flow rate was mixed with the product gases before entering the gas chromatography. The exact hydrogen production rate can be calculated by comparing the ratio of hydrogen to nitrogen because the flow rate of the carrier gas is known. The gas composition was detected by a TCD (thermal conductivity detector) with Ar as a reference gas. The product gas of the catalytic combustor was analyzed, after moisture was removed in a cold trap.

The energy balance between the methanol reformer and the catalytic combustor was calculated as shown in Table 2. The total heating energy consists of the energy to raise the reformer temperature and the heat of reaction. The heat of reaction is the sum of the reforming heat, the evaporation heat and the heat to raise mixture to reforming temperature (sensible heating). The energy to reform 1 mole methanol with 1 mole water is 158.3 kJ, which can be provided by burning 0.66 mole hydrogen by the catalytic combustor. The hydrogen can be provided by recycling the off-gas of the fuel cell. The reformer produces 2.7 moles hydrogen from 1 mole methanol when methanol conversion is 95% and hydrogen selectivity is 95%. Assuming that hydrogen utilization of the fuel cell is 72%, the amount of the hydrogen off-gas is 0.756 mole, which is greater than the hydrogen requiremnt for the combustor to sustain the reformer. Based on this calculation, the expected production of hydrogen is 54.5 ml/min when the methanol feed rate is 2 ml/h. The fuel cell consumes 72% portion (39.2 ml/min) in the reformed hydrogen and the remainder (15.3 ml/min) can be used to operate catalytic combustor.

|  | Calculation | Flow rate |
|---|---|---|
| Methanol input | 1 mol | 2 ml/h |
| Energy requirement for the reformer* | 153.8 kJ | |
| Evaporation and sensible heating of methanol | 48.4 kJ | |
| Evaporation and sensible heating of water | 51.5 kJ | |
| Heat of reaction | 58.4 kJ | |
| Expected production of hydrogen** | 2.7 mol | 54.5 ml/min |
| Hydrogen requirement for the combustor | 0.66 mol | 13.3 ml/min |
| Anode off-gas of fuel cell*** | 0.756 mol | 15.3 ml/min |

*Reforming temperature: 250 °C, **95% methanol conversion, 95% hydrogen selectivity, ***Fuel cell utilization: 72%

Table 2. Energy balance calculation between the methanol reformer and the combustor

### 2.4 Results and discussion

The performance of the reformer was measured at various test conditions and an optimum operation condition was sought. The measured performance of the reformer was expressed in terms of the methanol conversion, which is defined as follows:

$$\text{CH}_3\text{OH conversion [mol\%]} = \frac{\text{mol (CH}_3\text{OH)}_{\text{in}} - \text{mol (CH}_3\text{OH)}_{\text{out}}}{\text{mol (CH}_3\text{OH)}_{\text{in}}} \times 100 \qquad (4)$$

Figure 6 shows the methanol conversion as a function of the reformer temperature at each methanol feed rate with the steam-to-carbon ratio of 1.1. The methanol conversion decreased as the methanol feed rate increased, while the methanol conversion increased as the reformer temperature increased. The maximum methanol feed rate was 2 ml/h to obtain the methanol conversion higher than 90% at temperature lower than 250 ˚C. At the feed rate of 2 ml/h and the reformer temperature of 250 ˚C, the hydrogen production rate was 53.9 ml/min and the composition of carbon monoxide in the reformate gas was 0.49%.
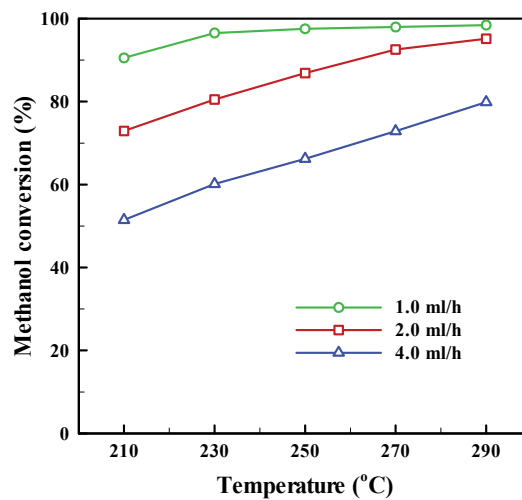


Fig. 6. Methanol conversion as a function of the reformer temperature

The performance of the catalytic combustor was measured at various conditions. Figure 7 shows the temperature variation of the catalytic combustor as a function of the reaction time at an equivalence ratio of 1.0. This plot includes the change of reformer temperature, which has to reach 250 ˚C to obtain the optimal methanol conversion. The temperatures of reformer and catalytic combustor were measured as varying the hydrogen feed rate. The air was mixed with hydrogen in the mixing chamber at the equivalent ratio of 1.0 and the gas mixture was fed into the combustor. In the energy balance calculation, the hydrogen requirement of the combustor was 15.3 ml/min to sustain the methanol reforming reaction at the methanol feed rate of 2 ml/h. At the feed rate of 15.3 ml/min, the temperature of the catalytic combustor reached 148.7 ˚C when 18 min elapsed after the initiation of the reaction. The hydrogen feed rate increased to reduce the time for the startup of the reformer. At the hydrogen feed rate of 41.3 ml/min, the combustor temperature reached 271 ˚C within 8.6 min after the start of operation and the reformer temperature was 250 ˚C. As the hydrogen feed rate increased, the combustion heat increased and the time for startup decreased. However, the hydrogen conversion decreased at the increase of the hydrogen feed rate due to the short residence time that is proportional to the inverse of the feed rate. Furthermore,

the hot-spot appeared in the fore part of the combustor, which can damage the catalyst and the reactor substrate. The temperature difference between the reformer and the combustor increased with the hydrogen feed rate. At the feed rate of 41.3 ml/min, the temperature difference was 21 ˚C when the reformer temperature reached 250 ˚C.
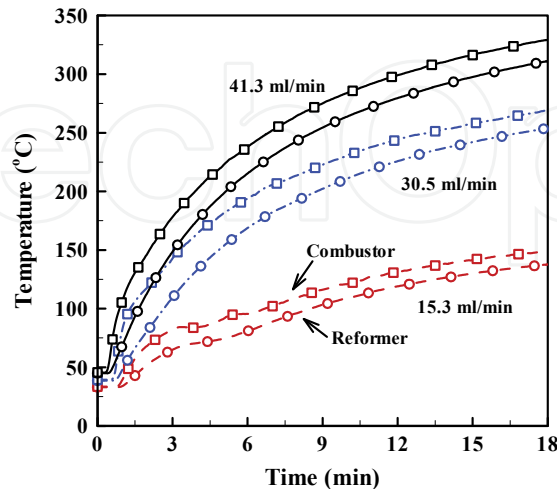


Fig. 7. Temperature variation of the catalytic combustor as a function of the reaction time.

Figure 8 represents the result of simultaneous operation of the methanol steam reformer and the catalytic combustor. The reformer was heated up to 250 ˚C by an external preheater with the increasing rate of temperature of 11.4 ˚C/min. The combustor was operated when the reformer temperature reached 250 ˚C. The hydrogen feed rate was 15.3 ml/min, which can be supplied from the anode off-gas of fuel cell when the methanol feed rate is 2 ml/h. The air was mixed with hydrogen to fix the equivalent ratio at 1.0. The methanol was fed into the reformer with the feed rate of 2 ml/h. The water feed rate was 0.98 ml/h to satisfy the steam-to-carbon ratio of 1.1. The reformer temperature was maintained constantly after the methanol reforming reaction was initiated. After 8 minutes into the simultaneous operation, steady reforming reaction was attained and the methanol conversion was higher than 90%. The maximum conversion of methanol was 95.7%. The temperature difference between the reformer and the combustor was approximately 4 ˚C.
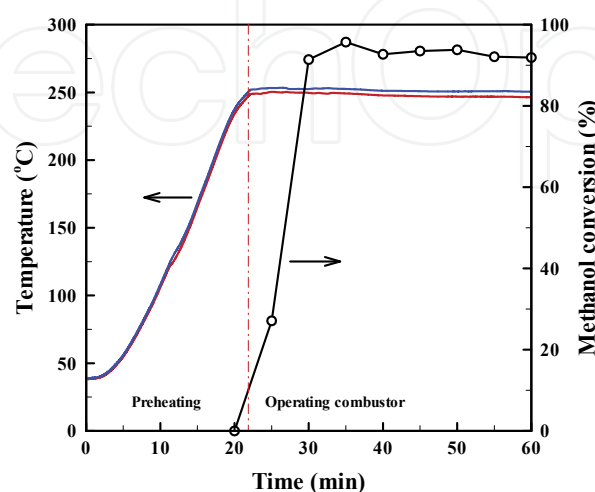


Fig. 8. Simultaneous operation of the methanol steam reformer and the catalytic combustor
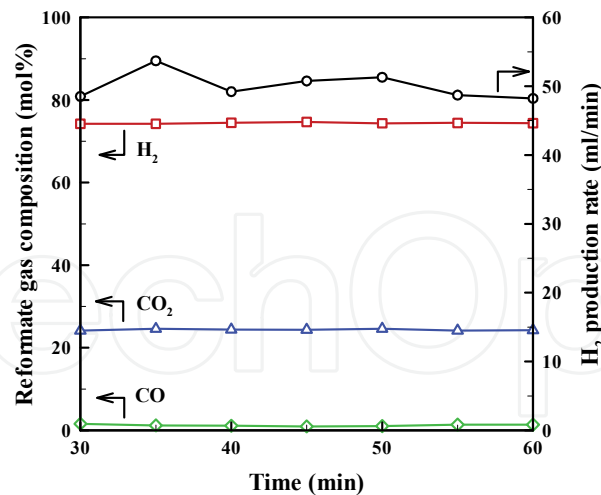
Fig. 9. The composition of reformate gas and the production rate of hydrogen

Figure 9 shows the composition of reformate gas and the hydrogen production rate after the start of complete operation. As the steady reforming reaction lasted, the composition of reformate gas remained constant. The reformate gas composition was 74.4% $H_2$, 24.36% $CO_2$, and 1.24% CO, and its flow rate was 67.2 ml/min. The hydrogen production rate was approximately 50 ml/min, which can generate 4.5 W electric power on a typical PEMFC. The concentration of carbon monoxide at the integrated test was higher than that at the separate test of the reformer. Although the catalytic combustor gave the sufficient amount of heat to operate the reformer, it could not form uniform temperature distribution within the reformer. As a result, the high temperature gradient occurred in the reformer, increasing the selectivity of carbon monoxide. The thermal efficiency of the conventional reformer combined with the combustor is defined by:

$$\eta_T = \frac{LHV_{H_2\_produced}}{LHV_{CH_3OH\_reformer} - LHV_{H_2\_combustor}} \times 100 \tag{5}$$

where the LHV means the lower heating value. The thermal efficiency of the integrated micro methanol reformer was 76.6%. The operating conditions and the performance of the micro methanol reformer is summarized in Table 3.

| Operating condition | Reformer | Combustor |
|---|---|---|
| Feed flow rate | 2 ml/h $CH_3OH$ | 15.3 ml/min $H_2$ |
| S/C (steam-to-carbon ratio) | 1.1 | |
| Equivalence ratio | | 1.0 |
| Temperature | 250 ˚C | 251 ˚C |
| Performance | Reformer only | Integrated operation |
| Temperature | | 247 ˚C (reformer) |
| Conversion | 96.2% | 95.7% |
| $H_2$ production rate | 53.9 ml/min | 50 ml/min |
| CO composition | 0.49% | 1.24% |
| Thermal efficiency | | 76.6% |

Table 3. The operating conditions and the performance of the micro methanol reformer

## 3. Micro reformer heated by hydrogen peroxide decomposition

### 3.1 Hydrogen peroxide as a heat source

In the previous section, the catalytic combustor is used as a heat source of the methanol steam reformer. However, it is still problematic that non-uniform distribution of reaction and hot spot formations in the fore region of the combustor. In the present study, the catalytic decomposition of hydrogen peroxide is used as a process to supply heat to the reformer. The decomposition reaction of hydrogen peroxide is expressed below:

$$H_2O_2 \rightarrow H_2O + 0.5 O_2, \quad \Delta H_f^o = -54.24 \, kJ/mol \tag{6}$$
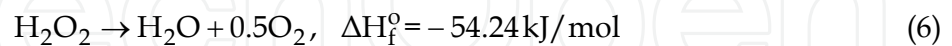
The construction of the micro methanol reformer complete with a heat source is presented in Fig. 10, in which the catalytic reactor for the hydrogen peroxide decomposition is included. The hydrogen peroxide decomposition is a highly exothermic reaction and generates the sufficient amount of heat to sustain the methanol steam reforming reaction. The catalytic decomposition of hydrogen peroxide has great reactivity and selectivity on various metal elements, such as Fe, Cu, Ni, Cr, Pt, Pd, Ir, and Mn (Teshima et al., 2004). The hydrogen peroxide decomposition generates steam and oxygen as products. The steam can be recycled into the reformer for the steam reforming reaction. The oxygen can be used as an oxidizer at the fuel cell cathode and to remove carbon monoxide in the preferential oxidation. The present concept renders the system far more compact than the existing reformer/combustor model because hydrogen peroxide is stored and used in condensed phase and oxygen enrichment enhances the system efficiency.

In the present study, the performance evaluation of the methanol steam reformer with hydrogen peroxide heat source was carried out at various test conditions and an optimum operation condition was sought.
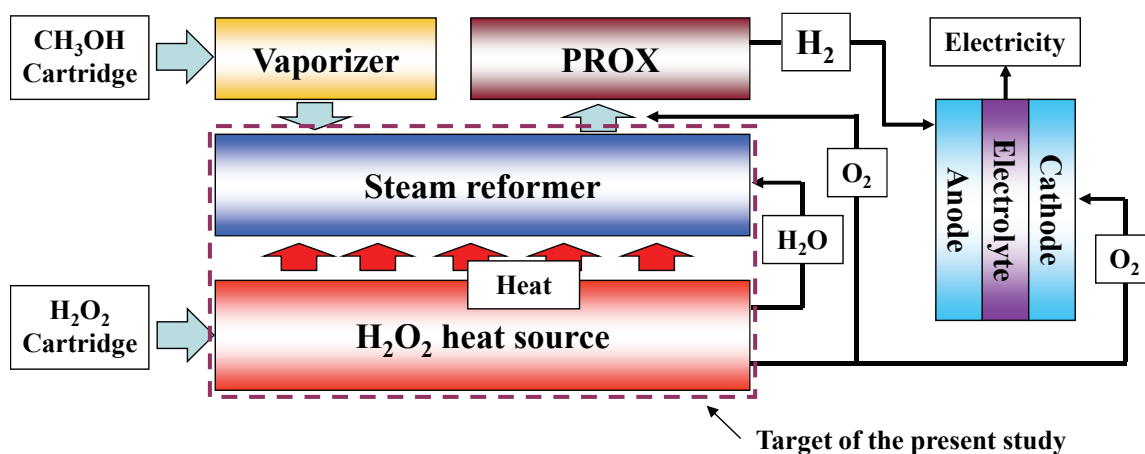


Fig. 10. Concept of methanol steam reformer integrated with hydrogen peroxide heat source

### 3.2 Experimental

Experimental apparatus for the performance measurement of the reformer system is similar with the combustor experiment. Two syringe pumps supplied reactants to the reactor at a controlled rate; one for the mixture of methanol and water, and the other for hydrogen peroxide. The temperature of each reactor was recorded by thermocouples. The analysis of the product gas composition was the same with the section 2.3. The concentration of

hydrogen peroxide was measured using a refractometer (PR-50HO, ATAGO) with a small quantity of sample. The product gas of hydrogen peroxide decomposition was analyzed, after moisture removed in a cold trap.

The measured performance of the reformer was expressed in terms of the methanol conversion, hydrogen selectivity and hydrogen peroxide conversion, which are defined as follows:
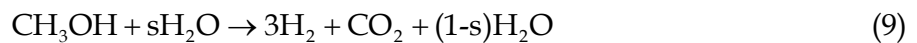
$$CH_3OH \text{ conversion [mol\%]} = \frac{\text{mol } (CH_3OH)_{in} - \text{mol } (CH_3OH)_{out}}{\text{mol } (CH_3OH)_{in}} \times 100 \tag{4}$$

$$H_2 \text{ selectivity [\%]} = \frac{\text{mol } (H_2) \times 1/3}{\text{mol } (CH_3OH)_{in} - \text{mol } (CH_3OH)_{out}} \times 100 \tag{7}$$

$$H_2O_2 \text{ conversion [mol\%]} = \frac{\text{mol } (H_2O_2)_{in} - \text{mol } (H_2O_2)_{out}}{\text{mol } (H_2O_2)_{in}} \times 100 \tag{8}$$

### 3.3 Operation parameter

The chemical equation of methanol steam reforming reaction is expressed below:

$$CH_3OH + sH_2O \rightarrow 3H_2 + CO_2 + (1\text{-}s)H_2O \tag{9}$$

where symbol s is the molal ratio of water to methanol ($H_2O/CH_3OH$), which is the same with the steam-to-carbon ratio. Decomposition reaction of hydrogen peroxide is expressed below:

$$a(xH_2O_2 + (1\text{-}x)H_2O)) \rightarrow 0.5axO_2 + (1 - x + ax)H_2O \tag{10}$$
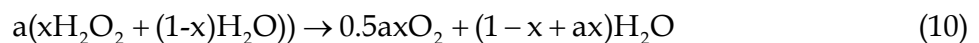
where symbol a and x are the molal ratio of hydrogen peroxide to methanol ($H_2O_2/CH_3OH$) and the molal concentration of hydrogen peroxide, respectively. The performance of the reformer system depends on these parameters. In order to determine the reaction condition, the concentration of hydrogen peroxide and the weight hourly space velocity (WHSV) were used as control parameters. The weight hourly space velocity indicates the ratio of the reactant flow rate to the catalyst mass as follows:

$$WHSV = \frac{\text{Molal flow rate of reactants (mol/h)}}{\text{Catalyst mass (g)}} \text{ [mol/g-h]} \tag{11}$$

Overall heat output of the integrated reformer system was calculated as shown in Fig. 11. Figure 11 (a) shows the variation in the decomposition reaction heat of hydrogen peroxide as a function of the weight concentration of hydrogen peroxide. It can be seen that the hydrogen peroxide concentration has to be higher than 73.9 wt % to generate the sufficient heat to complete the reforming reaction of methanol at s = 1.0 and a = 9.0, respectively. Hydrogen peroxide with even higher concentration is needed when the steam-to-carbon ratio is higher or the hydrogen peroxide-to-methanol ratio is lower.

Figure 11 (b) illustrates the net heat output that amounts to the difference between the decomposition heat of hydrogen peroxide and the heat required to maintain the reformer at the optimum operation condition. The decomposition heat of 5.3 moles hydrogen peroxide

at 81.5 wt % concentration releases the sufficient amount of heat to reform the mixture of 1 mole methanol and 1 mole water. The required amount of hydrogen peroxide will decrease when the hydrogen peroxide concentration increases or the steam-to-carbon ratio decreases. In the calculation that leaded to Fig. 11, the heat loss to the surrounding was ignored. Considering the heat loss of the reformer, higher concentration of hydrogen peroxide or higher hydrogen peroxide-to-methanol ratio is required. In the present study, hydrogen peroxide of 82 wt % concentration was used and the steam-to-carbon ratio was fixed at 1.1 for convenience in the experiment. The performance characteristics of the reformer was investigated with three control parameters; methanol space velocity, hydrogen peroxide space velocity, and hydrogen peroxiode-to-methanol ratio.
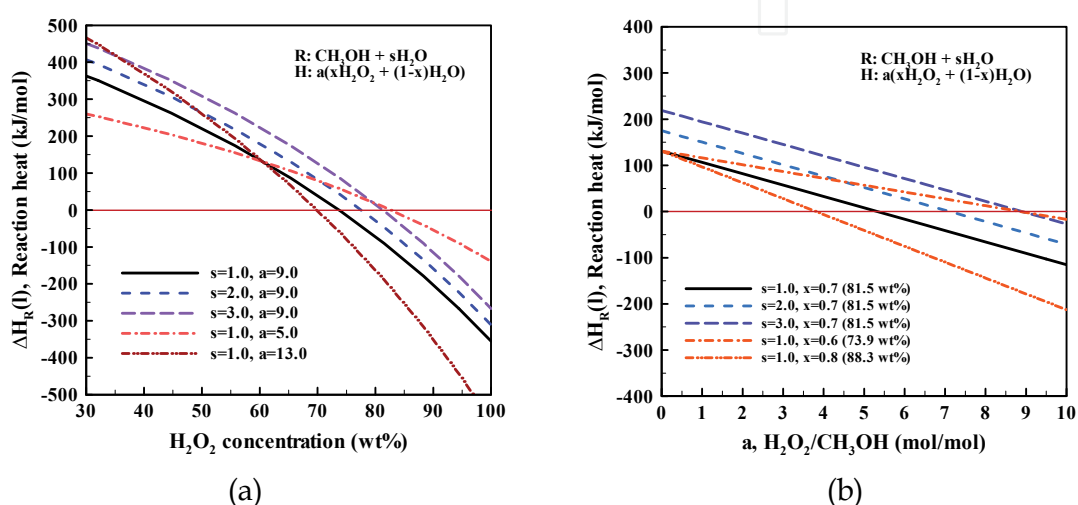


Fig. 11. Overall heat output of the integrated reformer system

### 3.4 Results and discussion

The temperature of the hydrogen peroxide decomposition reactor was measured as varying the hydrogen peroxide space velocity. Figure 12 (a) shows the temperature of the hydrogen peroxide decomposition reactor as a function of reaction time at each space velocity, in which the hydrogen peroxide conversion is included. At the space velocity of 6.32 mol/g-h, the hydrogen peroxide conversion was 98.2% and the reactor temperature reached 150 ˚C when 200 seconds elapsed after the initiation of reaction. At the space velocity of 37.3 mol/g-h, the reactor temperature reached 250 ˚C, which is the optimal temperature for the methanol reforming reaction, within a minute after the start of operation. The amount of reaction heat increases with the feed rate of hydrogen peroxide, reducing the time to obtain the optimal reformer temperature. At high space velocity, however, reactants does not take the residence time enough to react on the catalyst, resulting in the decrease of hydrogen peroxide conversion. At the low space velocity, the temperature difference between the reformer and the decomposition reactor was within 5 ˚C. At the space velocity of 37.3 mol/g-h, however, the temperature difference increased with the time after the start-up as shown in Fig. 12 (b). When the temperature of decomposition reactor reached 250 ˚C, the reformer temperature was less than 200 ˚C.

Figure 13 represents the simultaneous operation result of the methanol steam reformer and the hydrogen peroxide decomposition reactor. The reformer was heated up to 250 ˚C by the decomposition reactor with 82 wt% hydrogen peroxide at the space velocity of 9.48 mol/g-

h. The mixture of methanol and water was fed into the reformer with the steam-to-carbon ratio at 1.1. The space velocity of methanol was 0.68 mol/g-h. The temperature increased steadily after the methanol reforming reaction was initiated. It implies that the hydrogen peroxide feed rate exceeds the minimum to sustain the methanol reforming reaction. By reducing the feed rate down to the space velocity of 6.32 mol/g-h after 5 minutes into the operation, an ideal reaction condition was obtained as shown in Fig. 13. After 8 minutes into the operation, steady methanol reforming reaction was obtained and the methanol conversion was higher than 91.2%. The temperature inside the reformer and the decomposition reactor were 253 ˚C and 278 ˚C, respectively.



(a)                                                                                    (b)
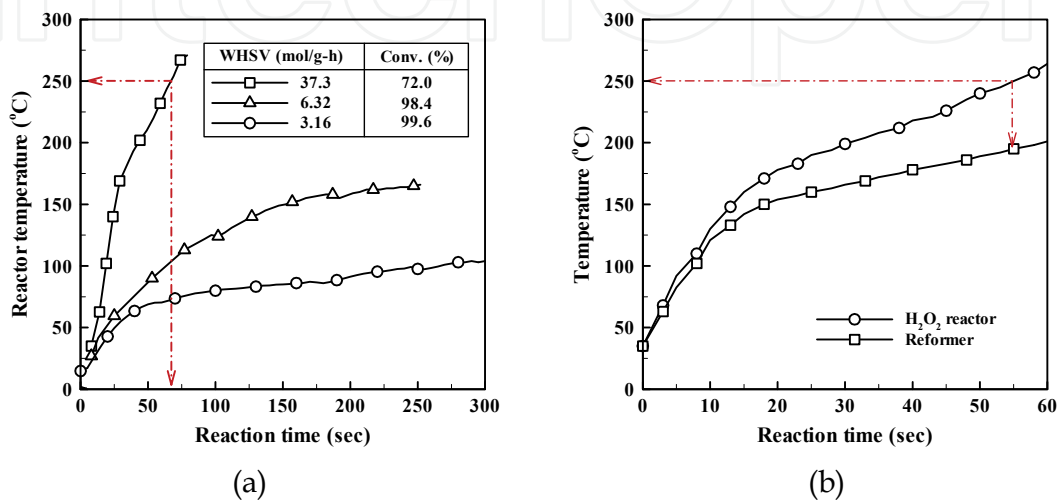
Fig. 12. The performance of hydrogen peroxide decomposition reactor
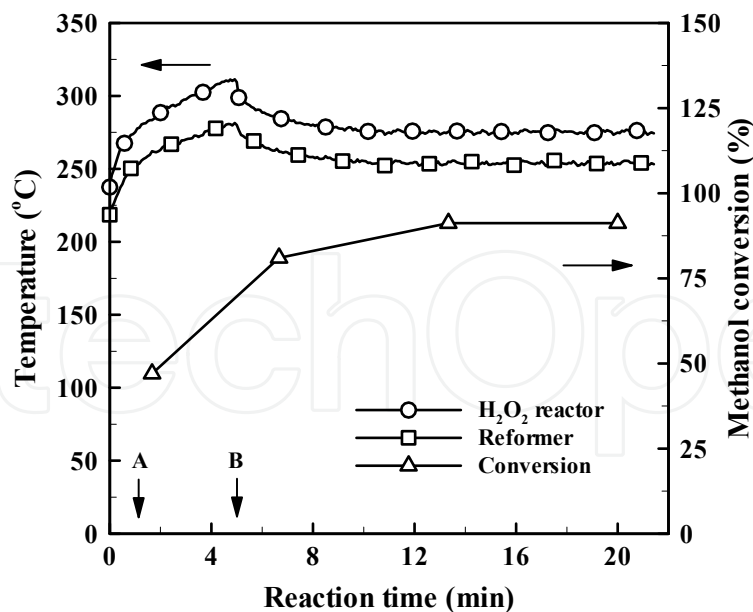


Fig. 13. Simultaneous operation of the micro reformer with hydrogen peroxide heat source

The performance characteristics of the micro reformer with hydrogen peroxide heat source was investigated at various conditions. Figure 14 (a) shows the effect of the methanol space velocity on the methanol conversion and the reformer temperature with the conditions of

the decomposition reactor fixed (S/C = 1.1, 82 wt% $H_2O_2$, $H_2O_2$ WHSV 6.32 mol/g-h). As the methanol space velocity increased, the reformer temperature decreased gradually because the hydrogen peroxide decomposition heat was consumed to vaporize the methanol supplied in liquid phase. As a result, the reformer decreased in temperature and did not sustain the methanol reforming reaction. Figure 14 (b) shows the effect of the reformer temperature on the methanol conversion. The feed rate of the methanol was fixed while the reformer temperature was determined by varying the feed rate of hydrogen peroxide ($CH_3OH$ WHSV 0.68 mol/g-h, S/C = 1.1, 82 wt% $H_2O_2$). The reformer temperature increased with the space velocity of hydrogen peroxide because the decomposition heat of hydrogen peroxide increased. The methanol conversion increased with the reformer temperature, when the temperature was below 250 ˚C. For the reformer temperature higher than 250 ˚C, the methanol conversion maintained its value at 250 ˚C.



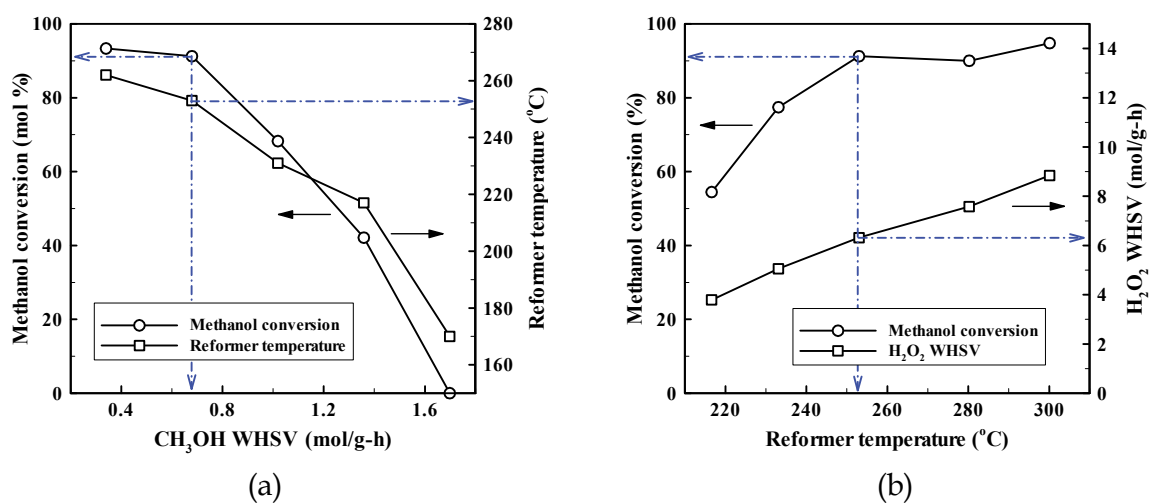(a)                                            (b)

Fig. 14. Performance characteristics of micro reformer with hydrogen peroxide heat source
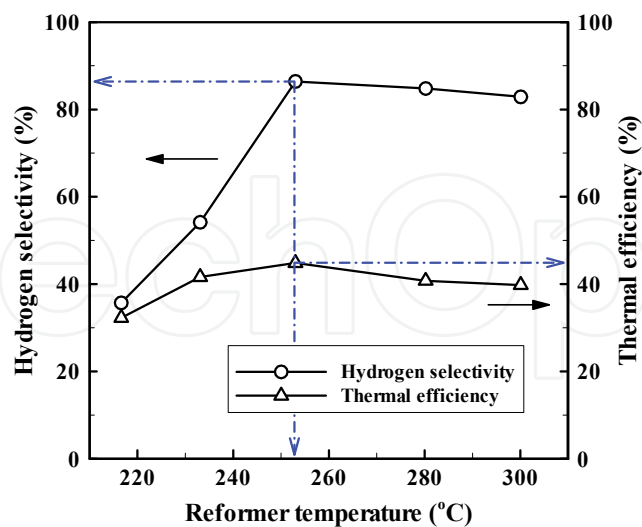


Fig. 15. Hydrogen selectivity and thermal efficiency as a function of reformer temperature

Figure 15 shows the hydrogen selectivity and the thermal efficiency of the system as a function of reformer temperature with the conditions of the reformer fixed. The thermal efficiency of the conventional reformer/combustor model is defined by:

$$\eta_T = \frac{LHV_{H_2\_produced}}{LHV_{CH_3OH\_reformer} - LHV_{H_2\_combustor}} \times 100 \qquad (5)$$

This formula could not be applied to the methanol reformer integrated with the hydrogen peroxide decomposition reactor, because the LHV of hydrogen peroxide is not defined. In the present study, the thermal efficiency for the reformer system is defined as follows:

$$\eta_T' = \frac{\Delta H^R_{H_2\_produced}}{\Delta H^R_{CH_3OH\_reformer} - \Delta H^R_{H_2O_2}} \times 100 \qquad (12)$$

The LHV was replaced with the heat of reaction. The LHV of hydrogen provided to the combustor in Eq. 5 was replaced with the decomposition heat of hydrogen peroxide. The hydrogen selectivity increased with the thermal efficiency as the reformer temperature increased. At the reformer temperature higher than 250 ˚C, however, the hydrogen selectivity decreased as the reformer temperature increased, because the production of carbon monoxide increased. The maximum hydrogen selectivity and the thermal efficiency were 86.4% and 44.8%, respectively. The product gas included 74.1% $H_2$, 24.5% $CO_2$ and 1.4% CO, and the total volume production rate was 23.5 ml/min. The hydrogen production rate is the sufficient amount to generate 1.5 W electrical power on a typical PEMFC. The optimum condition and the performance of the methanol reformer with hydrogen peroxide heat source are shown in Table 4.

The overall efficiency of typical PEMFC system using a methanol reformer is approximately 40% (Ishihara et al., 2004). In present study, the exergy loss can be reduced by the use of hydrogen peroxide decomposition reaction. The use of oxygen generated by the decomposition reaction raises the cell voltage, resulting in the increase of the fuel cell efficiency. It is understood that the overall efficiency of fuel cell system presented in present study is higher than that of the existing fuel cell model.

|                                  | $H_2O_2$ reactor | Reformer       |
|----------------------------------|------------------|----------------|
| Temperature                      | 278 ˚C           | 253 ˚C         |
| S/C (steam-to-carbon ratio)      |                  | 1.1            |
| $H_2O_2$ concentration           | 82 wt%           |                |
| Feed flow rate                   | 2 ml/h           | 10 ml/h        |
| WHSV                             | 0.68 mol/g-h     | 6.32 mol/g-h   |
| Conversion                       | 98.4 %           | 91.2 %         |
| $H_2$ production rate            |                  | 23.5 ml/min    |
| CO composition                   |                  | 1.4 %          |
| Hydrogen selectivity             |                  | 86.4%          |
| Thermal efficiency               |                  | 44.8%          |

Table 4. The optimum operation conditions and the performance of the integrated reformer

## 4. Integrated test with micro fuel cell

### 4.1 Removal of carbon monoxide

Removal of carbon monoxide from the reformate gas mixture is of paramount importance for development of a reformer in fuel cell applications because carbon monoxide deactivates

the anode catalyst of PEMFC. There are several processes for the carbon monoxide removal including pressure/temperature swing adsorption (PSA/TSA), methanation, membrane separation, and preferential oxidation. PSA/TSA are energy-intensive and expensive. Methanation consumes three moles of hydrogen to convert 1 mole CO into 1 mole methane as given below:

$$CO + 3H_2 \rightarrow CH_4 + H_2O \qquad (13)$$

It is therefore not recommended. The membrane separation is attractive method because high purity hydrogen can be obtained. PROX also is the preferred method because the small amount of oxygen is required to oxidize CO into $CO_2$ as expressed below:

$$CO + 1/2O_2 \rightarrow CO_2 \qquad (14)$$

### 4.2 Microreactor for preferential oxidation

Microreactor for PROX was prepared as shown in Fig. 16. Pt/Ru was selected as a catalyst of PROX. Microchannels were fabricated on a photosensitive glass.
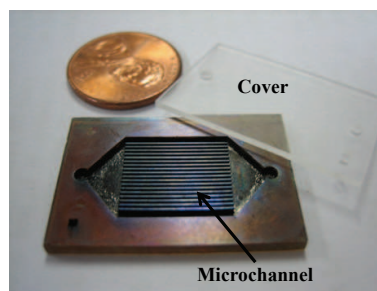


Fig. 16. Microreactor for preferential oxidation

As a washcoat layer, γ-Al$_2$O$_3$ was coated on the microchannels using sol-gel method and the catalyst was loaded by wet impregnation method. First, aluminum isopropoxide was hydrolyzed in deionized water with vigorous stirring for 1 hour at 80 ˚C. The sol was peptized by adding nitric acid (HNO$_3$) with adjusting the pH. Polyvinyl alcohol (PVA) solution was prepared by dissolving the PAV in deionized water at 75 ˚C. The presence of PVA can reduce crack formations of the washcoat layer at the drying time. The peptized sol and the PVA solution were mixed with adding the γ-Al$_2$O$_3$ powder to increase the concentration of γ-Al$_2$O$_3$ in the slurry. The mixture slurry was ball-milled for 72 hours. The glass substrate was then dipped into the prepared γ-Al$_2$O$_3$ slurry and dried for 2 hours at 120 ˚C after blowing off the excess slurry. This procedure was repeated to obtain the desired weight of the γ-Al$_2$O$_3$ washcoat layer. The washcoated microchannels were then calcined at 350 ˚C for 4 hours. A mixture of a 0.5 M aqueous solution of H$_2$PtCl$_6$ and a 0.5 M aqueous solution of RuCl$_3$ were prepared. The substrate was immersed in the mixture for 12 hours. The moisture was removed by drying the catalyst-loaded substrate in a convection oven at 70 ˚C for 12 hours. The calcination followed in a furnace at 350 ˚C for 3 hours. The catalyst was activated by reduction in a steady flowing hydrogen environment at 350 ˚C for 5 hours. The carbon monoxide conversion of PROX reactor as a function of the reaction temperature with varying the ratio of oxygen to carbon is shown in Fig. 17. Mixture gas including 69.91% H$_2$, 3.06% CO, 2.03% CH$_4$, and 25% CO$_2$ was used in the test of PROX reactor. The carbon monoxide conversion increased with the oxygen-to-carbon ratio and the reactor

temperature. In the case of 5 wt% Pt/Ru/γ-Al$_2$O$_3$ catalyst, the carbon monoxide was removed completely with oxygen-to-carbon ratio of 4 at 200 ˚C.
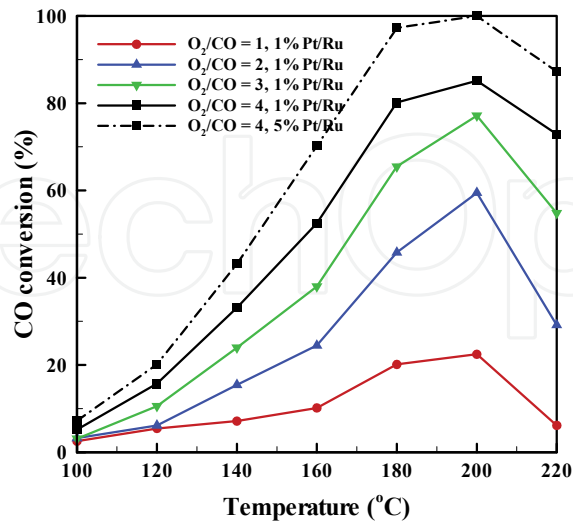


Fig. 17. Conversion of carbon monoxide of PROX microreactor

## 4.3 Integrated test with micro fuel cell

MEMS fuel cell was fabricated for integrated tests with the micro reformer. The structure of the micro fuel cell is shown in Fig. 18. Membrane electrode assembly (MEA) was prepared by coating 0.3 mg/cm² Pt-Ru/C for an anode catalyst and 0.3 mg/cm² Pt/C for a cathode catalyst on a Nafion-112 membrane. The reason to select Pt-Ru/C as an anode catalyst is because Pt/C is poisoned by carbon monoxide in the reformate gas even if removed via PROX reaction. Carbon paper (TGP-H-090, 260 μm) was used as a gas diffusion layer (GDL). Flow channels were fabricated by etching the photosensitive glass wafer, on which the current collectors, Ag/Ti layer, were sputtered. Overall fabrication process is presented in Fig. 18 and the fabricated micro fuel cell is shown in Fig. 19.
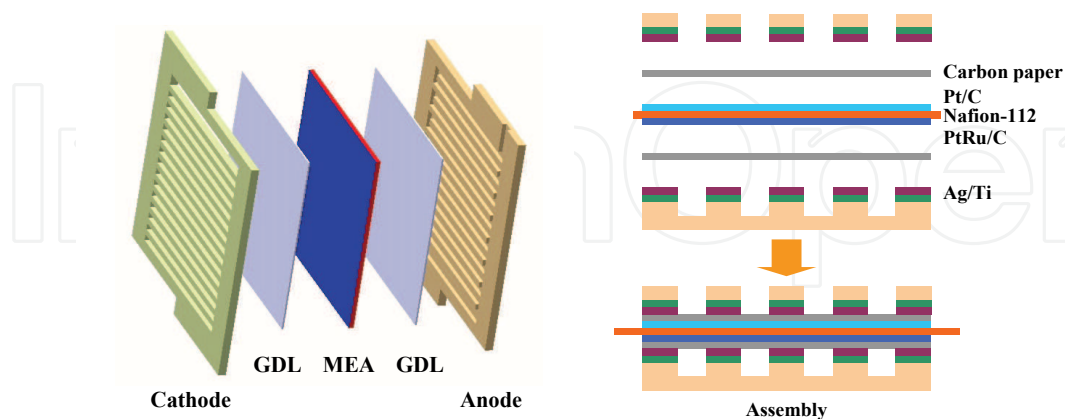


Fig. 18. Structure and fabrication process of MEMS fuel cell

Experimental layout for integrated tests of the reformer with the micro fuel cell is shown in Fig. 20. The micro fuel cell was tested with pure hydrogen to compare with the result with the reformate gas. Simultaneous operation of the micro reformer, PROX reactor, and micro fuel cell was carried out.
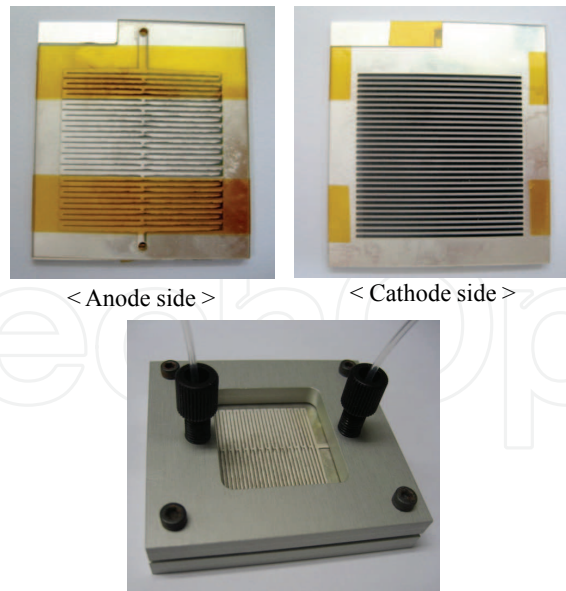
< Anode side >          < Cathode side >
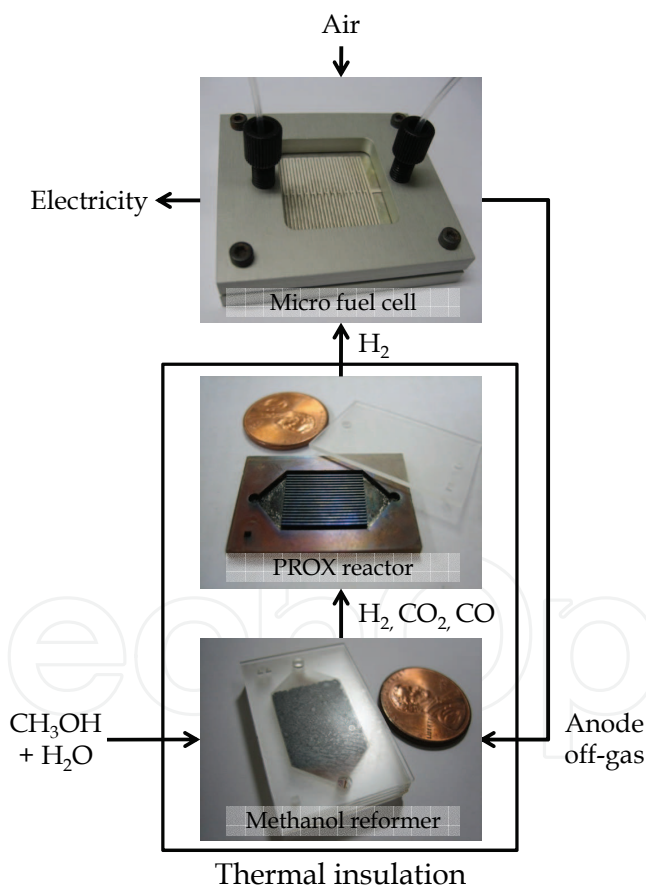


Fig. 19. Fabricated results of the micro fuel cell



Fig. 20. Schematic of the integrated test of micro reformer-PROX reactor-micro fuel cell

## 4.4 Results and discussion

Performance of MEMS fuel cell system with pure hydrogen and the reformate gas is shown in Fig. 21. Pure hydrogen gas feed rate was set in 50 ml/min. When methanol feed rate was

2 ml/h, the flow rate of reformate gas was 71.96 ml/min. The reformate gas included 74.4% hydrogen, thus the hydrogen flow was 53.5 ml/min. The power density was 184 mW/cm² when the potential was 0.64 V. The performance was low compared with the result for pure hydrogen due to the feed at the fuel cell that included undesired CO, $CO_2$, and $N_2$.
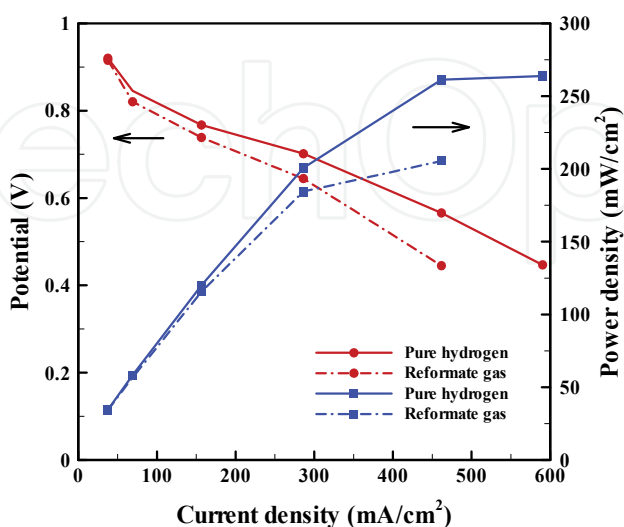


Fig. 21. Performance curve of MEMS fuel cell system

Specific energy density of the micro fuel cell system was calculated to compare with the state-of-art batteries. First, the overall energy budget for operation of the fuel cell system was calculated. Figure 22 presents the energy specification of each reaction step.
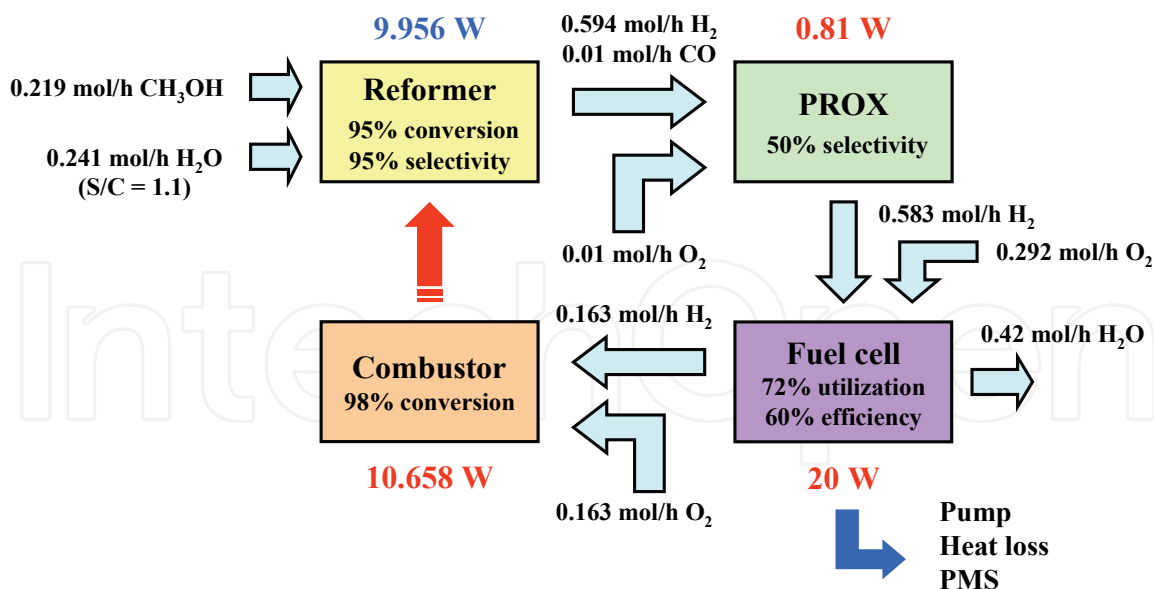


Fig. 22. Energy budget for a fuel cell system

The 20 W fuel cell system requires the hydrogen of 0.42 mol/hr. Thus, methanol feed rate of 0.219 mol/hr is required, assuming 95% methanol conversion and 95% hydrogen selectivity of the reformer. The energy requirement of the reformer consists of sensible heat, vaporization heat, and endothermic reforming reaction heat as given below:

$$\int_{298}^{338} C_{p,CH_3OH(l)} dT + \int_{338}^{523} C_{p,CH_3OH(g)} dT + \Delta H_{CH_3OH}^v$$
$$+ \int_{298}^{373} C_{p,H_2O(l)} dT + \int_{373}^{523} C_{p,H_2O(g)} dT + \Delta H_{H_2O}^v + \Delta H_{523}^R \qquad (15)$$

The total energy input for the methanol reformer is 9.956 W. The catalytic combustor generates 10.658 W heat energy with the fuel cell off-gas of 0.163 mol/hr, which is greater than the reformer energy requirement. It means that the fuel cell system can be operated without the additional heat supply to sustain the methanol reforming reaction.

The methanol storage of 4.386 moles is required for the duration of 20 hours (0.219 mol/hr × 20 hr). The water feed requirement is 0.241 mol/hr at the steam-to-carbon ratio of 1.1, thus the water storage is 4.825 moles (0.241 mol/hr × 20 hr). These translate into 140.49 g (178.97 cc) methanol, and 87.093 g (87.25 cc) water, respectively. Therefore, the net fuel mixture storage requirement would be 227.58 g or 266.22 cc.

The specifications of the fabricated fuel cell are: mass of 0.5 g, volume of 2.7 cc, active area of 4 cm², and power density of 180 mW/cm². Thus 20 W fuel cell would have a mass of 13.89 g (0.5 g × 20 W / (0.18 W/cm² × 4 cm²)) and a volume of 75 cc. The specific power density of the micro reformer was 0.34 W/g or 1.25 W/cc. The reformer would have a mass of 59.62 g and a volume of 16 cc for 20 W fuel cell to be operated in the sufficient hydrogen supply. Therefore, the mass and volume of the total system were 301 g and 357 cc, respectively.

The energy storage capacity was 400 W·hr (20 W × 20 hr). So, the fuel cell system would have a weight specific energy density of 1329 W·hr/kg and a volume specific energy density of 1120 W·hr/L, which are values 10 times higher than the state-of-art of rechargeable batteries. The system energy density as the duration is shown in Fig. 23. The water production rate in the fuel cell was 0.42 mol/hr, which is greater than the water supply of the reformer (0.241 mol/hr) as shown in Fig. 22. Thus, the water from the fuel cell can be recycled into the reformer, improving the system energy densities. The specific energy densities for 10 days duration would be 2728 W·hr/kg and 2144 W·hr/L, respectively. It means that the micro fuel cell system can be an ideal alternative solution for portable micro power sources in the future.
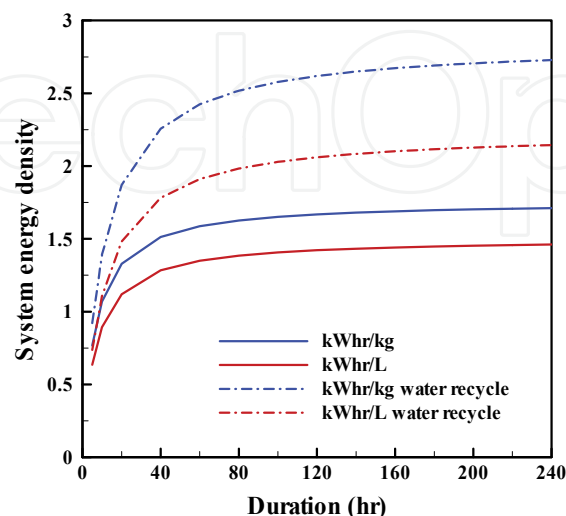


Fig. 23. System energy density as a function of the duration

## 5. Conclusion and future research

### 5.1 Conclusion

The design, fabrication and performance evaluation of micro methanol reformer integrated with a heat source were described in this chapter. The micro methanol reformer consists of the steam reformer, the catalytic combustor, and the heat exchanger in-between. The two heat sources for the reformer were used; one is the hydrogen catalytic combustion and the other is the hydrogen peroxide decomposition.

All reactions, the methanol reforming reaction, the hydrogen combustion, and the hydrogen peroxide decomposition, are the catalytic process. $Cu/ZnO$ was used for the reformer and Pt for the catalytic combustor. The porous ceramic material was used as the catalyst support to enhance the catalytic surface area. The catalytic microreactor was fabricated on five photosensitive glass wafers; top and bottom covers, a reformer layer with $Cu/ZnO$/support insert, a combustor layer with Pt/support insert, and a heat exchanger layer in-between.

The performance of the reformer complete with the catalytic combustor was measured. The methanol conversion was 95.7%, and the thermal efficiency was 76.6%. The reformate gas flow including three major elements, 74.4% $H_2$, 24.36% $CO_2$, and 1.24% $CO$ was 67.2 ml/min. The hydrogen flow in the reformate gas was the sufficient amount to run 4.5 W PEMFC.

The performance characteristics of the methanol reformer with the hydrogen peroxide heat source was investigated. The methanol conversion over 91.2% and the hydrogen selectivity over 86.4% were obtained. A modified thermal efficiency using the reaction heat of hydrogen peroxide instead of the LHV was defined and the thermal efficiency of the system was 44.8%. The reformate gas flow including 74.1% $H_2$, 24.5% $CO_2$ and 1.4% $CO$ was 23.5 ml/min. This hydrogen was the sufficient amount to run 1.5 W PEMFC. The performance of the present methanol reformer can be further enhanced by using hydrogen peroxide with higher concentration.

The microreactor for the PROX reaction was fabricated using the photosensitive glass process integrated with the $Pt/Ru/\gamma\text{-}Al_2O_3$ sol-gel coating process. The carbon monoxide in the reformate gas was removed to use directly in the micro fuel cell.

The micro fuel cell was fabricated and connected with the micro reformer and PROX reactor.

The power density of the micro fuel cell system was 184 mW/cm² at the potential of 0.64 V and is lower than that in the case of pure hydrogen test, because the reformate gas included the undesired $CO$, $CO_2$, and $N_2$.

The system energy density of the micro fuel cell system integrated with the methanol reformer was calculated. The overall energy budget was calculated to operate the reformer-combined fuel cell system. The system energy storage density of the micro fuel cell system was obtained in the range of 1329 W·hr/kg to 2728 W·hr/kg. It is estimated that the micro fuel cell combined with the micro reformer has the energy density of up to 10 times higher than existing batteries, thus expecting to appear in the mobile energy market of the future.

### 5.2 Future research

Although the integrated methanol reformer developed in the present study can be used directly to operate the micro fuel cell, several works may be continued such as a fully integrated microfabrication, thermal packing, and optimization.

The micro reformer should be insulted thermally to obtain the high thermal efficiency and the low package temperature of the micro fuel cell system. The excess heat loss of the

reformer makes the catalytic combustor difficult to sustain the methanol reforming reaction. The thermal insulation of the reformer facilitates the integration of the reformer with the micro fuel cell at the low package temperature. The heat loss through conduction and convention can be prevented by the vacuum packaging technology using an anodic bonding process. The thermal design of the micro reformer through the extensive modeling of the heat transfer will be preceded to improve the overall thermal efficiency of the micro fuel cell system.

The fully integrated microfabrication of the micro fuel cell system is the next challenge to improve the system packaging efficiency. The batch fabrication of all elements including the micro reformer, PROX reactor, and micro fuel cell can reduce the fabrication cost. The overall integrated design of the micro fuel cell system should be optimized in consideration of the thermal balance and fluidic interconnections between the reactors. The micropump, microvalve, and control circuitry will be integrated with the micro reformer and micro fuel cell in the future.

## 6. Notation

| | |
|---|---|
| a | Molal ratio of hydrogen peroxide to methanol |
| $C_p$ | Constant pressure specific heat, kJ/mol-K |
| LHV | Lower heating value, kJ/mol |
| $O_2/C$ | Oxygen-to-carbon ratio |
| S/C | Steam-to-carbon ratio |
| s | Molal ratio of water to methanol |
| WHSV | Weight hourly space velocity, mol/g-h |
| x | Molal concentration of hydrogen peroxide |
| $\eta_T$ | Thermal efficiency |
| $\Delta H^R$ | Heat of reaction, kJ/mol |
| $\Delta H^V$ | Vaporization heat, kJ/mol |

## 7. References

Agrell, J.; Boutonnet, M. & Fierro, J. (2003). Production of hydrogen from methanol over binary Cu/ZnO catalysts Part II. Catalytic activity and reaction pathways, *Applied Catalysis A: General*, Vol. 253, pp. 213–223, 0926-860X

Delsman, E.; De Croon, M.; Pierik, A.; Kramer, G.; Cobden, P.; Hofmann, C.; Cominos, V. & Schouten, J. (2004). Design and operation of a preferential oxidation microdevice for a portable fuel processor, *Chemical Engineering Science*, Vol. 59, pp. 4795-4802, 0009-2509

Holladay, D.; Wainright, S.; Jones, O. & Gano, R. (2004). Power generation using a mesoscale fuel cell integrated with a microscale fuel processor, *Journal of Power Sources*, Vol. 130, pp. 111–118, 0378-7753

Ishihara, A.; Mitsushima, S.; Kamiya, N. & Ota, K. (2004). Exergy analysis of polymer electrolyte fuel cell systems using methanol, *Journal of Power Sources*, Vol. 126, pp. 34–40, 0378-7753

Kim, T. & Kwon, S. (2006a). Design, fabrication and testing of a catalytic microreactor for hydrogen production, *Journal of Micromechenics and Microengineering*, Vol. 16, pp. 1752–1760, 0960-1317

Kim, T. & Kwon, S. (2006b). Preparation of Cu/ZnO for Fabrication of a Micro Methanol Reformer, *Chemical Engineering Journal*, Vol. 123, No. 3, pp. 93-102, 1369-703X

Kim, T.; Hwang, J. & Kwon, S. (2007). A MEMS methanol reformer heated by decomposition of hydrogen peroxide, *Lab on a Chip*, Vol. 7, No. 7, pp. 836–847, 1473-0197

Kundu, A.; Jang, J.; Lee, H.; Kim, S.; Gil, J.; Jung, C. & Oh, Y. (2006). MEMS-based micro-fuel processor for application in a cell phone, *Journal of Power Sources*, Vol. 162, pp. 572–578, 0378-7753

Lindstrom, B. & Pettersson, L. (2001). Hydrogen generation by steam reforming of methanol over copper-based catalysts for fuel cell applications, *International Journal of Hydrogen Energy*, Vol. 26, pp. 923–933, 0360-3199

Lindström, B.; Agrell, J. & Pettersson, L. (2003). Combined methanol reforming for hydrogen generation over monolithic catalysts, *Chemical Engineering Journal*, Vol. 93, pp. 91–101, 1369-703X

Lua, G.; Wang, C.; Yen, T. & Zhang, X. (2004). Development and characterization of a silicon-based micro direct methanol fuel cell, *Electrochimica Acta*, Vol. 49, pp. 821–828, 0013-4686

Nguyen, N. & Chan S. (2006). Micromachined polymer electrolyte membrane and direct methanol fuel cells—a review, *Journal of Micromechanics and Microengineering*, Vol. 16, pp. R1–R12, 0960-1317

O'Hayre, R.; Cha, S.; Colella, W. & Prinz, F. (2006). *Fuel Cell Fundamentals*, pp. 10-11, John Wiley & Sons, Inc., 978-0-471-74148-0, New York

Pattekar, A. & Kothare, M. (2004). A Microreactor for Hydrogen Production in Micro Fuel Cell Applications, *Journal of Microelectromechical Systems*, Vol. 13, No. 1, pp. 7-18, 1057-7157

Pattekar, A. & Kothare, M. (2005). A radial microfluidic fuel processor, *Journal of Power Sources*, Vol. 147, pp. 116–127, 0378-7753

Schuessler, M.; Portscher, M. & Limbeck, U. (2003). Monolithic integrated fuel processor for the conversion of liquid methanol, *Catalysis Today*, Vol. 79–80, pp. 511–520, 0920-5861

Teshima, N.; Genfa, Z. & Dasgupta, P. Catalytic decomposition of hydrogen peroxide by a flow-through self-regulating platinum black heater, *Analytica Chimica Acta*, Vol. 510, pp. 9–13, 0003-2670

Wang, Z.; Xi, J.; Wang, W. & Lu, G. (2003). Selective production of hydrogen by partial oxidation of methanol over Cu/Cr catalysts, *Journal of Molecular Catalysis A: Chemical*, Vol. 191, pp. 123–134, 1381-1169

Yamazaki, Y. (2004). Application of MEMS technology to micro fuel cells, *Electrochimica Acta*, Vol. 50, pp. 663–666, 0013-4686

Yoshida, K.; Tanaka, S.; Hiraki, H. & Esashi, M. (2006). A micro fuel reformer integrated with a combustor and a microchannel evaporator, *Journal of Micromechanics and Microengineering*, Vol. 16, pp. S191–S197, 0960-1317
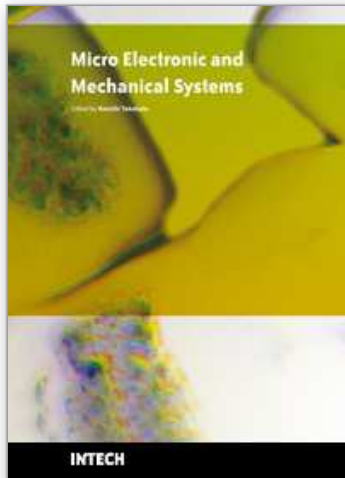
**Micro Electronic and Mechanical Systems**

Edited by Kenichi Takahata

This book discusses key aspects of MEMS technology areas, organized in twenty-seven chapters that present the latest research developments in micro electronic and mechanical systems. The book addresses a wide range of fundamental and practical issues related to MEMS, advanced metal-oxide-semiconductor (MOS) and complementary MOS (CMOS) devices, SoC technology, integrated circuit testing and verification, and other important topics in the field.  Several chapters cover state-of-the-art microfabrication techniques and materials as enabling technologies for the microsystems. Reliability issues concerning both electronic and mechanical aspects of these devices and systems are also addressed in various chapters.

**How to reference**

In order to correctly reference this scholarly work, feel free to copy and paste the following:

Taegyu Kim (2009). Micro Power Generation from Micro Fuel Cell Combined with Micro Methanol Reformer, Micro Electronic and Mechanical Systems, Kenichi Takahata (Ed.), ISBN: 978-953-307-027-8, InTech, Available from: http://www.intechopen.com/books/micro-electronic-and-mechanical-systems/micro_power_generation_from_micro_fuel_cell_combined_with_micro_methanol_reformer

# INTECH
open science | open minds